AEA/RS R4389

AEA Technology
Materials and Chemistry Division

The Electrical Conductivity of Sapphire Irradiated at 550-700°C

G P Pells and B C Sowden

5 May 1993

Work undertaken for the European Office of Aerospace Research and Development of the USAF under Contract Number F61708 92 C0043

AEA Technology
Materials and Chemistry Division
B393/1.21, Harwell, Didcot
Oxfordshire OX11 0RA
United Kingdom
Telephone 0235 434735
Facsimile 0235 435941

REPORT DOCUMENTATION PAGE

Form Approved OMB No. 0704-0188

1. AGENCY USE ONLY (Leave blank)	2. REPORT DATE	3. REPORT TYPE AND DATES COVERED
	5 May 1993	Final Report

4. TITLE AND SUBTITLE

The Electrical Conductivity of Sapphire Irradiated at 550-700°C

5. FUNDING NUMBERS

F6170892C0043

6. AUTHOR(S)

Dr. G. Phillip Pells

7. PERFORMING ORGANIZATION NAME(S) AND ADDRESS(ES)

AEA Technology
Materials and Chemistry Division
B393/1.21, Harwell, Didcot
Oxfordshire OX11 0RA, UK

8. PERFORMING ORGANIZATION REPORT NUMBER

AEA/RS R4389

9. SPONSORING/MONITORING AGENCY NAME(S) AND ADDRESS(ES)

EOARD
PSC 802 BOX 14
FPO 09499-0200

10. SPONSORING/MONITORING AGENCY REPORT NUMBER

SPC-92-4030

11. SUPPLEMENTARY NOTES

12a. DISTRIBUTION/AVAILABILITY STATEMENT

Approved for public release; distribution is unlimited.

12b. DISTRIBUTION CODE

A

13. ABSTRACT (Maximum 200 words)

The effects of radiation on electrical conductivity in ceramic insulators are briefly reviewed with particular emphasis on the radiation-induced electrical degradation (RIED) effect in which large increases in the intrinsic electrical conductivity have been observed following irradiation within a restricted temperature range whilst subject to electric fields > 600V/cm. The aim of the present work was to extend the studies of the RIED effect to temperatures relevant to thermionic fuel elements in space power systems such as TOPAZ II.

14. SUBJECT TERMS

15. NUMBER OF PAGES

17

16. PRICE CODE

17. SECURITY CLASSIFICATION OF REPORT	18. SECURITY CLASSIFICATION OF THIS PAGE	19. SECURITY CLASSIFICATION OF ABSTRACT	20. LIMITATION OF ABSTRACT
UNCLASSIFIED	UNCLASSIFIED	UNCLASSIFIED	UL

ABSTRACT

The effects of radiation on electrical conductivity in ceramic insulators are briefly reviewed with particular emphasis on the radiation-induced electrical degradation (RIED) effect in which large increases in the intrinsic electrical conductivity have been observed following irradiation within a restricted temperature range whilst subject to electric fields >600V/cm. The aim of the present work was to extend the studies of the RIED effect to temperatures relevant to thermionic fuel elements in space power systems such as TOPAZ-II.

The experimental arrangement using the Harwell Tandem accelerator is described along with the target which is capable of operating at temperatures up to 900C in a vacuum of $< 10^{-6}$ mbar. Irradiations were performed on sapphire at 550, 600, 650 and 700C using 10MeV protons to damage doses of $>10^{-3}$ displacements per atom (dpa). An electric field of 1kV/cm was applied across the sample during irradiation. The irradiations were interrupted at intervals and the temperature dependence of electrical conductivity measured. The experimental results showed that for irradiation temperature $>$ 600C the conductivity decreased with increasing damage dose. Irradiation at 600C produced more complex changes in which the conductivity depended upon both the damage dose and the thermal history of the sample. The conductivity initially decreased after a dose of 10^{-4}dpa but began to increase again after 10^{-3}dpa. However, holding at 500C overnight annealed out the increase and the conductivity fell back to the earlier decreasing trend line. Irradiation at 550C produced an order of magnitude increase in conductivity although, as at 600C, there was still a tendency for the increased conductivity to anneal out.

It is concluded that this work supported previous observations that the RIED effect does not occur in sapphire at temperatures above 550C but does not exclude the possibility that the defects responsible for the instabilities in the conductivity at 550/600C may become stable under different irradiation conditions and lead to the RIED effect.

Contents

1 Introduction

2 Experimental Methods

2 The Irradiation Facility

2 The High Temperature Target

3 Experimental Procedure

4 Experimental Results

5 Discussion

6 Conclusions

7 References

1. INTRODUCTION

The effects of ionising radiation on the electrical conductivity of insulators is reasonably well understood and has been discussed by Van Lint [1] and Pells [2]. The radiation-induced conductivity (RIC) is not necessarily a linear function of ionising dose rate and it has been shown for alumina that the RIC is best described by a power law with a dose rate exponent that can be greater or less than unity, depending upon the irradiation temperature. Quantitative data for the dose rate exponent and constants of proportionality have been given by Pells et al [3,4,5,6]. Recently Hodgson [7,8,9,10,11] has shown that when alumina is simultaneously exposed to a moderate electric field, moderate temperature and radiation damage, the intrinsic conductivity may increase by many orders of magnitude. This has been termed radiation-induced electrical degradation (RIED). The electric field may be ac or dc [11] with a major threshold occurring at ~ 700V/cm. Degradation still occurs with lower electric fields but after a much longer incubation time. Both ionisation and displacement damage appear to be necessary features [7] and RIED has been observed within the temperature range 300-500C. The effect occurs at lower temperatures but over longer time scales. Hodgson used 1.8MeV electrons but the effect has also been seen with proton and neutron irradiations. Pells [12] irradiated alumina with 18MeV protons at 400 and 500C with an applied electric field of 5kV/cm. Permanent increases in the conductivity occurred for the 500C irradiation only, although the increase was very large giving a conductivity of ~ 10^{-3}S/m after a damage dose of 2.5 x 10^{-3}dpa. Similar changes were reported by Ivanov et al [13] for neutron irradiations at 445C.

The onset of degradation occurs after ~10^{-5}dpa for both electron and proton irradiations and has saturated after ~10^{-2}dpa. These are very low doses in radiation damage terms. There is no generally accepted model for the RIED effect but it appears to be associated with the formation of aluminium colloids [9] which can be of sufficient size to be seen with an optical microscope. The temperature range over which RIED occurs (300-500C) suggests that diffusion on the oxygen sublattice is involved as aluminium Frenkel pairs are practically immobile below 400C. This is supported to some extent by the observation [10] that there is an enhanced production of F^+ centres (an oxygen vacancy with one trapped electron) during irradiation with an applied electric field, although how this leads to nucleation of aluminium colloids after a dose of 10^{-5}dpa remains unclear.

The original aim of the work was to determine the radiation damage dose and the electric field threshold required to degrade alumina insulators exposed to conditions expected in a General Atomics type thermionic fuel element. This was to be achieved by measuring the electrical conductivity of alumina exposed to 10MeV proton irradiation at temperatures of 700-750C and electric fields of 400-1000V/cm. As will be seen in the following sections the first irradiation to be performed at 700C and 1000V/cm demonstrated that degradation did not occur for damage doses up to 10^{-2}.

2. EXPERIMENTAL METHODS

2.1 The Irradiation Facility

The target assembly was built on the end of one of the beam lines attached to the Tandem accelerator equipped with full beam steering and focusing lenses and operating at a base vacuum pressure of $< 1 \times 10^{-6}$mbar. The Tandem accelerator has a maximum proton beam energy of 12MeV and a beam current of ~ 5uA. The target assembly consisted of two major sections. The first was a collimator box pumped by a 280l/s diffusion pump. The collimator consisted of four air cooled quadrants which defined a 10mm diameter aperture. The beam current on each quadrant could be monitored individually. A water cooled beam stop could be inserted immediately after the quadrants and was used for setting up the irradiation beam. The quadrant box was separated from the target chamber by a 300mm long, 25mm diameter tube to provide a measure of differential pumping between the two sections.

The specimen chamber was 450mm long by 150mm diameter with five major ports plus two small ports for vacuum gauges and two angled ports for observation of the target area. A second set of quadrants was mounted at the beam entry port. The chamber was pumped by a 1000l/s cryopump giving $\sim 10^{-8}$mbar base pressure and $< 10^{-7}$mbar during proton irradiation with the sample at 700C. The conductivity target was mounted on the end port and the whole of the target chamber was insulated from earth so that the target sample could be used as a Faraday cup to measure beam current. In practise irradiation with an electric field applied to the sample made it impossible to measure beam current directly and the current had to be measured by periodically inserting the beam stop into the proton beam during the course of an irradiation. The ratio of the target current to the beam stop current was determined before the irradiation started. The 10MeV proton beam was adjusted to give a slightly divergent beam such that a small fraction of the beam was stopped by each of the 8 quadrants. Correct alignment of the proton beam was maintained by ensuring that equal currents were maintained on all of the quadrants. The divergent beam also ensured that the beam flux across the target face did not vary by more than 20%.

2.2 The High Temperature Target

The sample holder had to compromise between being able to dissipate the irradiating beam power at low irradiation temperatures and yet allow the sample to be heated to high temperatures when required. Movement of the sample relative to the beam, and the electrical constraints due to thermal expansion, also had to be minimised. This was achieved by arranging for the sample to be carried on a heater supported inside a nest of stainless steel tubes coaxial with the irradiating beam as shown in Figure 1. The far end of the heater was air cooled to protect the vacuum seals and the whole heater was filled with helium gas. A controlling chromel-alumel thermocouple ran up the centre of the heater to within 1mm of the sample. On test the heater was run up to 900C and the

vacuum pressure in the chamber returned to $< 10^{-6}$ mbar after initial outgassing.

The sapphire samples were ground and polished to a thickness of 0.25mm. Platinum electrodes, 200nm thick, were evaporated onto both polished surfaces with a mask on one side providing a 10mm diameter central electrode and a guard ring. The other side was bonded to a larger diameter platinum disc by hot pressing overnight at 1000C with a thin gold disc between them. The platinum disc carrying the sapphire sample was edge clamped to the stainless steel sample holder.

Electrical contacts to the centre and guard electrodes of the sample were made by tungsten springs carried by a MACOR glass plate supported by three stainless steel tubes. The three tubes also served as the electrical shields for the leads between the tungsten springs and the leadthroughs on the main vacuum flange which also carried the heater.

2.3 Experimental Procedure

Prior to irradiation the sample was heated to 700C and held at that temperature to outgas the system. The electrical conductivity was also measured during the warming and cooling cycles. During the course of the work it was found that the conductivity varied with thermal cycling before irradiation. This feature of the sapphire samples was not explored in detail but on the second half of the programme the samples were thermally cycled several times before conductivity measurements were made.

As mentioned before the 10MeV proton beam was set up to give a slightly divergent beam just touching all eight segments of both collimators. A final collimator 9.5mm diameter was positioned 30mm in front of the target sample. This stopped the annular space between the centre electrode and guard ring of the sample from being irradiated and so prevented a stable and possibly conducting layer forming from residual organic gases in the vacuum system and bridging the inner and outer electrodes during the long irradiations.

Once the beam had been set up an electric field of 1kV/cm was applied across the thickness of the sample and the irradiation was started. The change in sample temperature due to beam heating was monitored by an infra-red thermometer and the heater controller adjusted to give the required irradiation temperature. Beam heating produced temperature increases of 20-30C with proton beam powers of 10-30W/cm^2. The beam heating increased during the course of an irradiation as the thermal conductivity of the sample decreased due to radiation damage. This was compensated for by adjusting the set point of the temperature controller and the nominal irradiation temperature was held to $\pm$ 10C throughout an irradiation. The beam current was monitored on the first collimator flap every half hour but rarely varied by more than 10% of the original setting during the course of a day's irradiation. The irradiation was interrupted every hour and the temperature dependence of conductivity

measured over the range 500-700C with the irradiating proton beam off. This procedure was changed for the irradiation at 550C for reasons that will be discussed later: measurements were made at the irradiation temperature only, not over a temperature range.

3. EXPERIMENTAL RESULTS

Irradiation at 700C produced a large decrease in conductivity with increasing dose as shown in Figure 2(a) where it can be seen that the decrease occurs over a wide temperature range. The activation energy for electrical conductivity at 700C was 2.0eV in the unirradiated material but can be seen to decrease to ~1.5eV after a damage dose of $9x10^{-3}$dpa. The change in conductivity at 700C as a function of damage dose is given in Figure 3 in a log/log plot. It can be seen that the conductivity begins to decrease after a damage dose greater than 10^{-4} dpa and has reduced by more than a factor 100 by 10^{-2}dpa. Irradiation at 650C showed similar behaviour as illustrated in Figure 2(b) and Figure 3 although the conductivity was not reduced by such a large factor.

Irradiation at 600C produced a greater variability in the temperature dependence measured after each irradiation period. Although the conductivity decreased after 10^{-4}dpa, as for the higher irradiation temperatures, there was a qualitative difference in the Arrhenius plots in that the log of conductivity was a simple linear function of reciprocal temperature instead of the curves obtained for the higher irradiation temperatures. The activation energy for electrical conductivity for the results given in Fig.4(b) was ~2.6eV for damage doses up to $1.7x10^{-3}$dpa. However, at higher doses more complex behaviour was observed and the Arrhenius plots began to deviate from linearity at temperatures below the irradiation temperature as shown in Fig.4(b). The details of the conductivity varied with the thermal history and reference to Fig.5 will show that the conductivity measured at the irradiation temperature was higher than those that had undergone thermal cycling, and those measured during the course of a heating cycle were higher than those measured during the course of a cooling cycle that had started at 700C. Measurements at 600C after holding overnight at 500C showed large reductions in conductivity in line with the trend shown after the lower dose irradiations.

As a result of the apparent annealing behaviour associated with temperature cycling during the conductivity measurements described above it was decide to limit the conductivity measurements in the final irradiation at 550C to the irradiation temperature alone, i.e. 550C. The results are given in Fig.6 where it can be seen that there was a very rapid increase in conductivity by a factor of ~10 after which the conductivity showed little change up to $2x10^{-3}$dpa. The conductivity decreased after holding overnight at 350C but increased up to near the previous days value with continued irradiation. The temperature dependence of electrical conductivity was measured at the beginning and end of each day's irradiation and is shown in Fig.7.

4. DISCUSSION

The experimental results obtained in the present study have been surprisingly complex in comparison with previous work at Harwell on polycrystalline alumina [2,3,5,6,12] where the measurements have been highly reproducible and gave simple temperature dependencies. However, the complex temperature dependencies shown in Figs 4(b) and 7 are similar to those reported by Klaffky et al [14] for sapphire from two suppliers Adolf Mellor and Co (Verneuil) and Union Carbide (Czochralski), which in neither case gave linear Arrhenius curves. It was concluded that the conductivity was controlled by a high concentration of shallow traps. Klaffky [15] also measured the conductivity of a sapphire sample that had been fast neutron irradiated to a fluence of $\sim 3 \times 10^{20} n/cm^2$ at ~150C and subsequently annealed at 1150C for 30 minutes. It was found that the conductivity decreased by almost three orders of magnitude. Examination by TEM showed a high density of small dislocation loops.

The large decrease in conductivity observed at 650C and 700C in the present work may be associated with the number of vacancies on the lattice. These tend to be high at these temperatures because interstitials are being stabilised in interstitial dislocation loops and hence reduce vacancy interstitial recombination. As the temperature is reduced below 600C defect diffusion rates are reduced but vacancy concentrations may also be reduced because of an increase in interstitials available for vacancy interstitial recombination as they no longer aggregate into dislocation loops so easily. Below 500C vacancy concentrations rise again as long range diffusion rates decrease still further. However, at temperatures between 300C and 500C the monovacancies tend to form aggregates which may provide the nuclei for the aluminium colloids observed in the RIED phenomena.

It can be seen in Figure 5 that irradiation to doses $> 10^{-3}$dpa at 600C reversed the trend towards decreasing conductivity with increasing damage dose and the conductivity began to rise. However, this condition appeared to be unstable as holding the sample overnight at 500C led to a return to a decreasing conductivity in line with the trend at lower doses. A similar tendency was observed for irradiation at 550C although in this case the overnight holding temperature was 350C less annealing was produced. Irradiation at 550C increased the conductivity above that of the starting material, but not to the same degree as observed by Pells [12] or Hodgson [10,11] at slightly lower temperature. This may be consistent with the temperature dependence of the RIED effect as given by Hodgson [10] who found that the effect peaked at ~470C. The proton irradiation by Pells [12], seemed to require a slightly higher irradiation temperature to produce a given increase in conductivity. Therefore, the increases in conductivity found in the present work may be associated with the nucleation of aluminium colloids which, because of the higher temperatures, do not reach a stable size and are constantly redissolving whenever the irradiating beam is switched off to make a measurement. Whether this be the case or not the results confirm the observation that the RIED effect only occurs over a narrow temperature range of ~ 200C.

The results of this study may also have been influenced by the electric field (1kV/cm). this was a factor of 5 less than that used by Pells [12] who found a large degradation at 500C. Although Hodgson [11] found that the electric field had a threshold of 600V/cm at 450C it is possible that the threshold is temperature dependent and the value of 1kV/cm used here could be below the primary threshold. Further work would be needed to resolve this question.

5. CONCLUSIONS

- Irradiation of sapphire with 10MeV protons at temperatures $>$600C while subject to an electric field of 1kV/cm produces a decrease in electrical conductivity for damage doses $> 10^{-4}$dpa.

- Similar irradiation at temperatures $<$ 600C may lead to an increase in electrical conductivity but the changes are unstable and tend to anneal out when the irradiation ceases.

- Variations in electric field or dose rate for irradiations at temperatures up to 600C may lead to stabilisation of defect nuclei leading to the RIED effect.

REFERENCES

[1] V A G van Lint, J M Bunch and T M Flanagan in Proc. Int. Conf on Radiation Effects and Tritiun Technology for Fusion Reactors, USERDA Report CONF 750989 (1976) pII-498

[2] G P Pells, J Nucl Mater, 155-157 (1988) 67

[3] G P Pells, S N Buckley, P Agnew, A J E Forman, M J Murphy and S A B Staunton-Lambert, AERE -R13222 (1988)

[4] G P Pells, S N Buckley, G J Hill and M J Murphy, AERE-R11715 (1985)

[5] G P Pells, Radiat Effects, 97 (1986) 199

[6] G P Pells, and G J Hill, J Nucl Mater, 141-143 (1986) 375

[7] E R Hodgson, Cryst Latt Defects in Amorphous Mater, 18 (1989) 169

[8] E R Hodgson, J Nucl Mater, 179-181 (1991) 383

[9] E R Hodgson, Radiat Eff Defects Solids, 119-121 (1991) 827

[10] E R Hodgson, Nucl Instrum and Methods in Phys Res B, 65 (1992) 298

[11] E R Hodgson, J Nucl Mater., 191-194 (1992) 552

[12] G P Pells, J Nucl Mater, 184 (1991) 177

[13] V M Ivanov, G M Kalinin, V F Kuzovitkin, SP Sklizkov, N V Morkina, VV Sarksyan and V A Skobeleva, Inorg Mater., 17 (1981) 1203

[14] R W Klaffky, B H Rose, A N Goland and G J Diennes, Phys Rev B, 21 (1980) 3610

[15] R W Klaffky, DOE/ER-0048/1 UC20, 21 (1980) 19

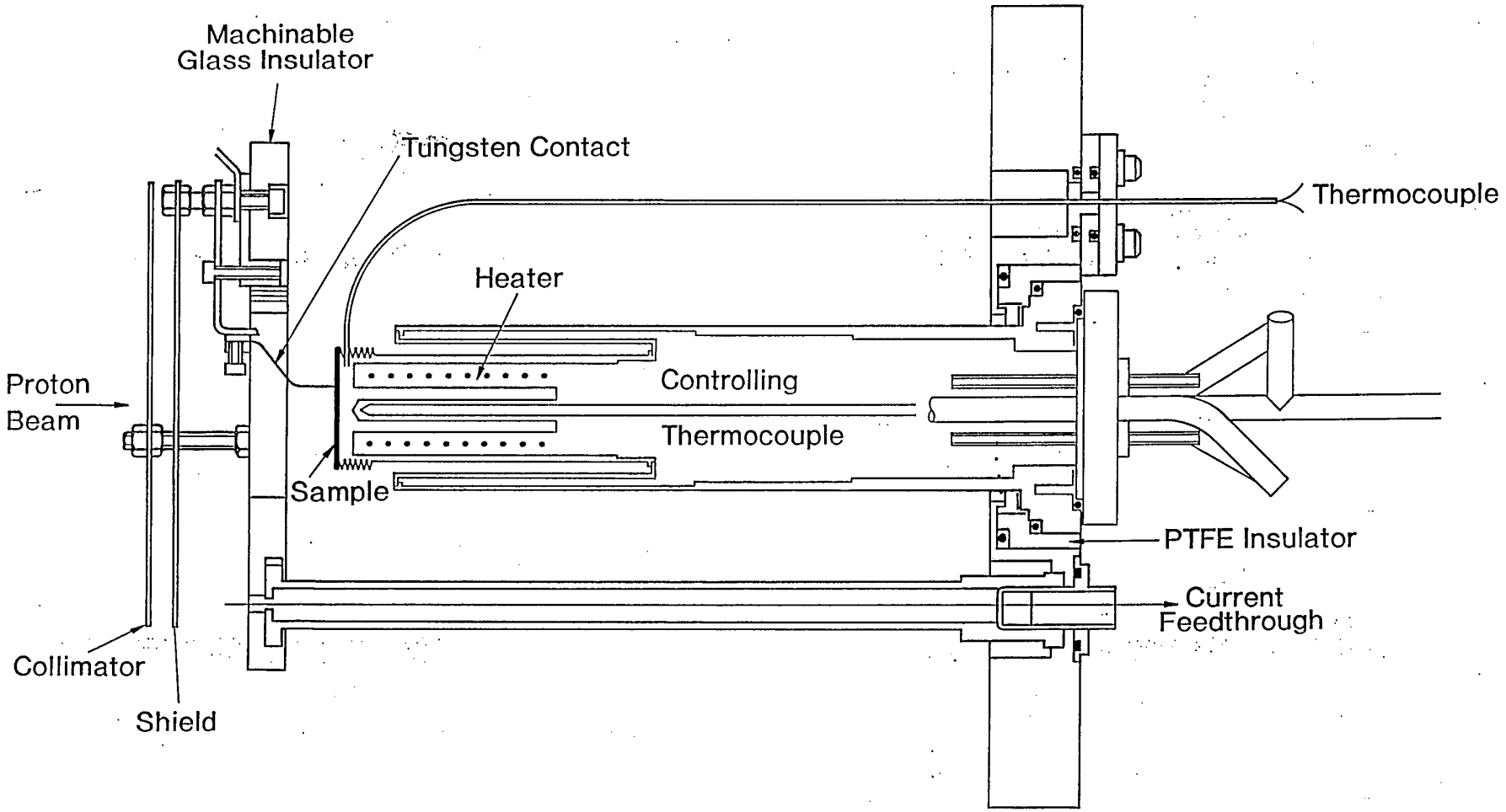

Fig. 1.
Cross section of target assembly

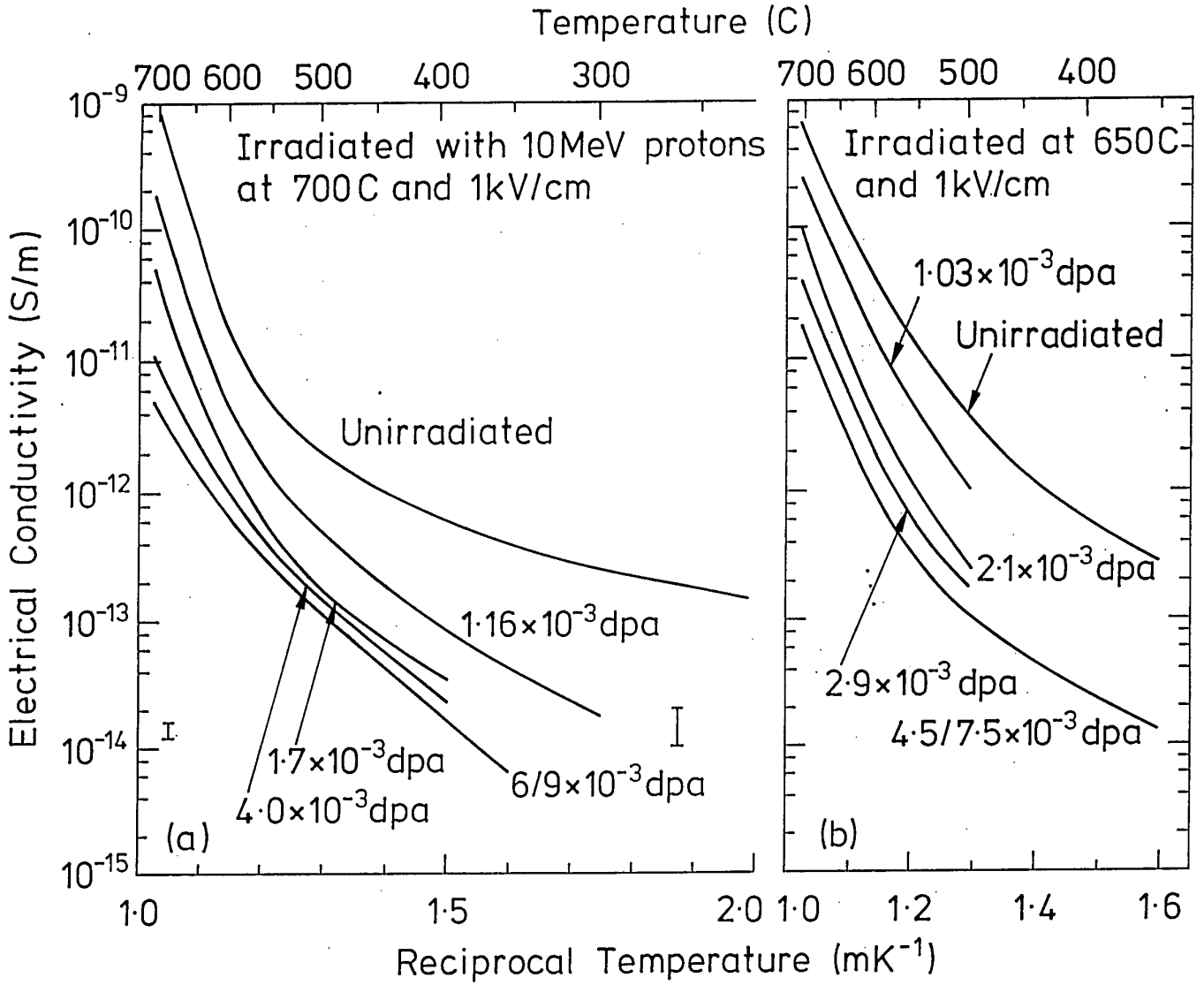

Fig. 2.
The intrinsic electrical conductivity as a function of temperature after 10MeV proton irradiation to the indicated damage doses at (a) 700C and (b) 650C with an applied electric field of 1kV/cm.

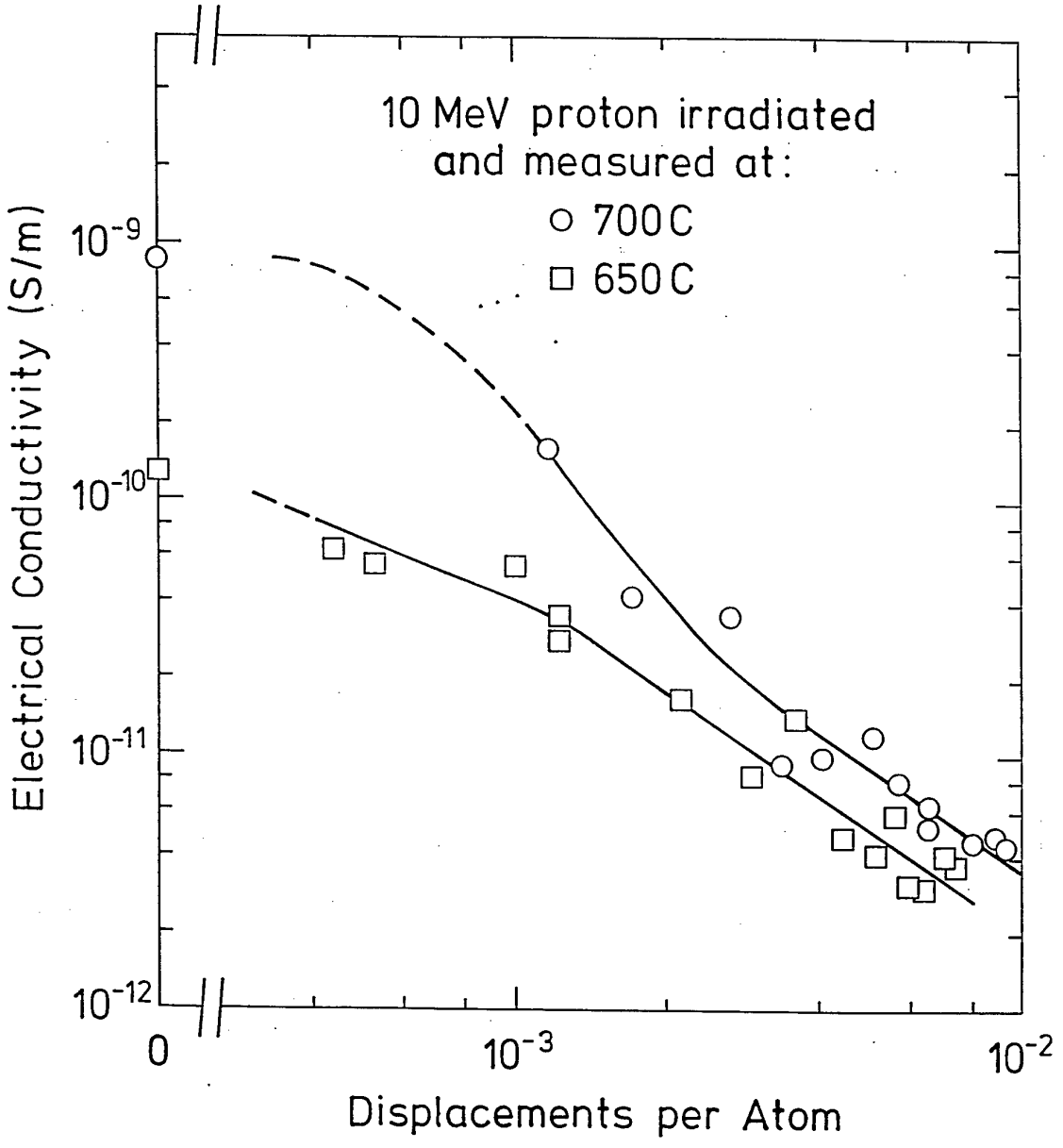

Fig. 3.
The intrinsic electrical conductivity as a function of damage dose after proton irradiation at the indicated temperatures with an applied electric field of 1kV/cm.

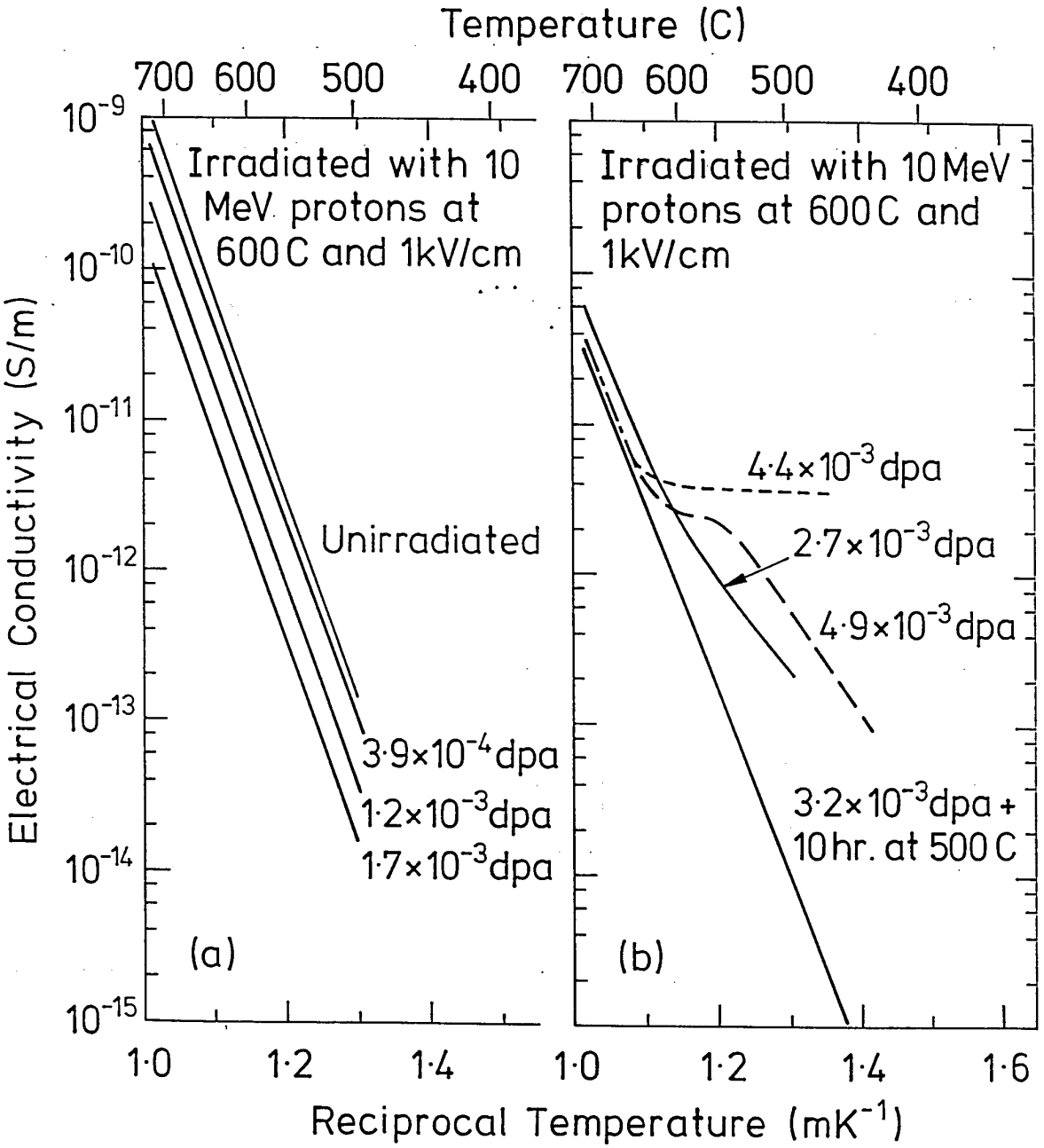

Fig. 4.
The intrinsic electrical conductivity as a function of temperature after proton irradiation to the indicated damage doses at 600C.

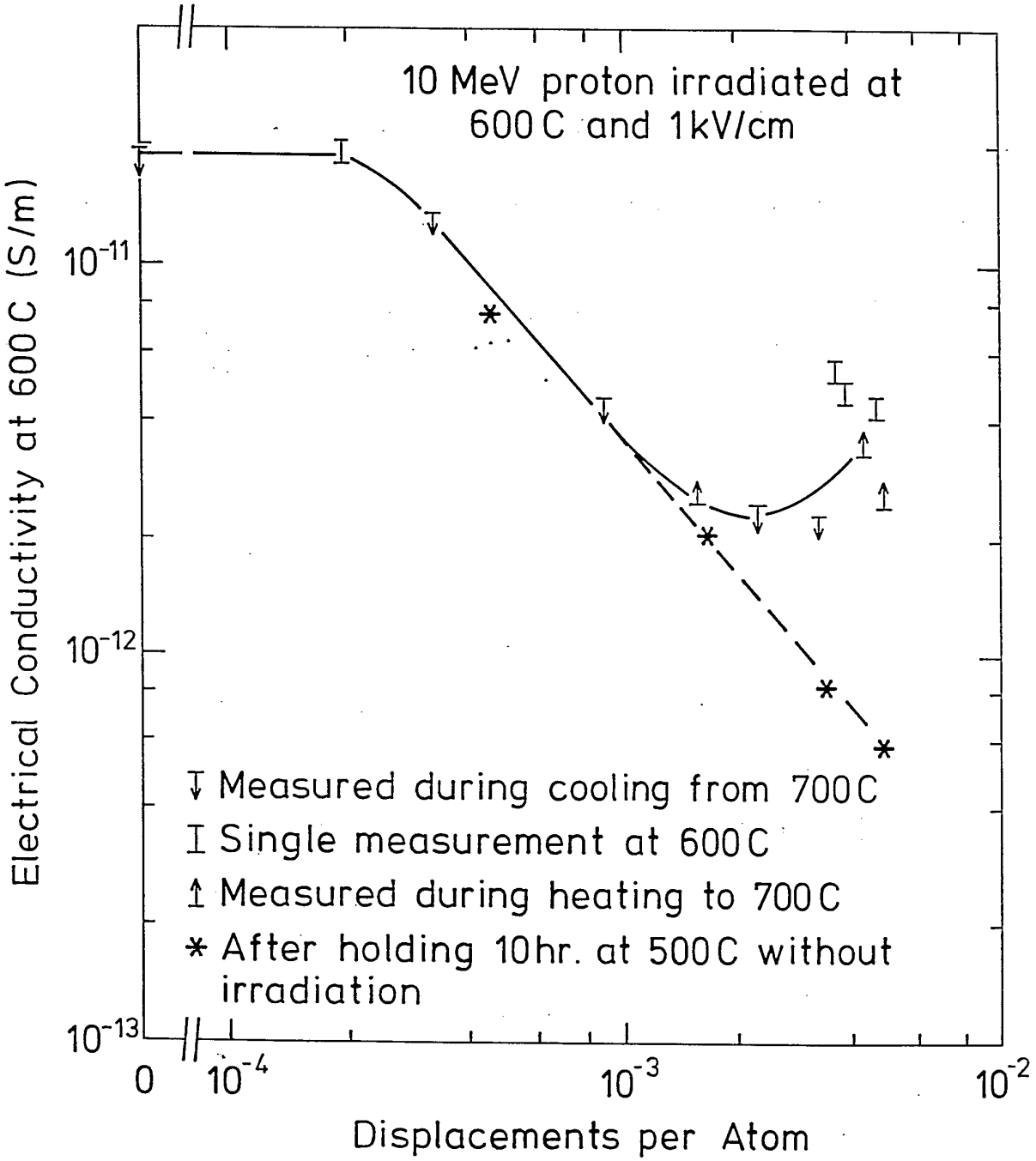

Fig. 5.
The intrinsic electrical conductivity as a function damage dose for various thermal cycles.

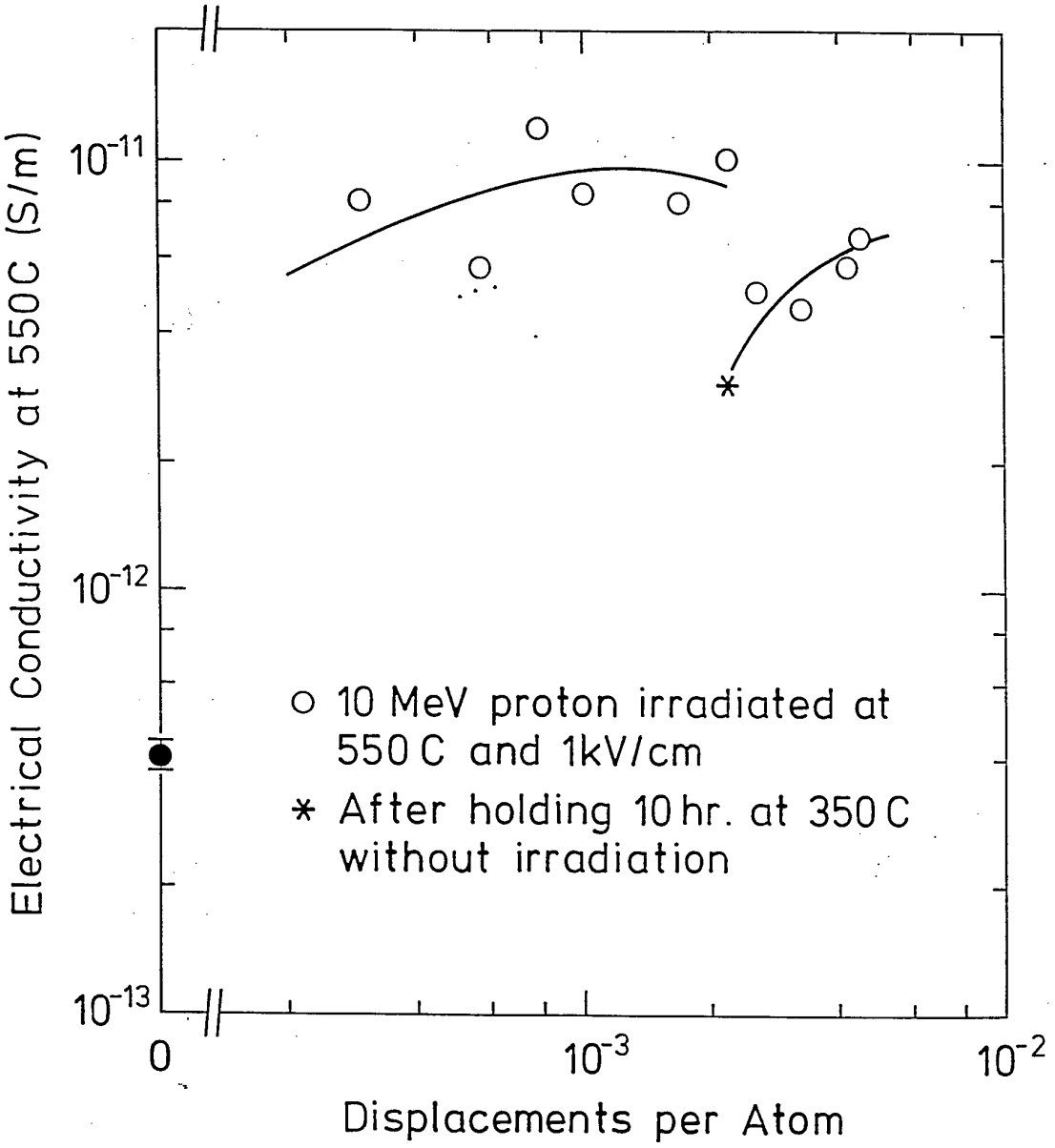

Fig. 6.
The intrinsic electrical conductivity as a function of damage dose

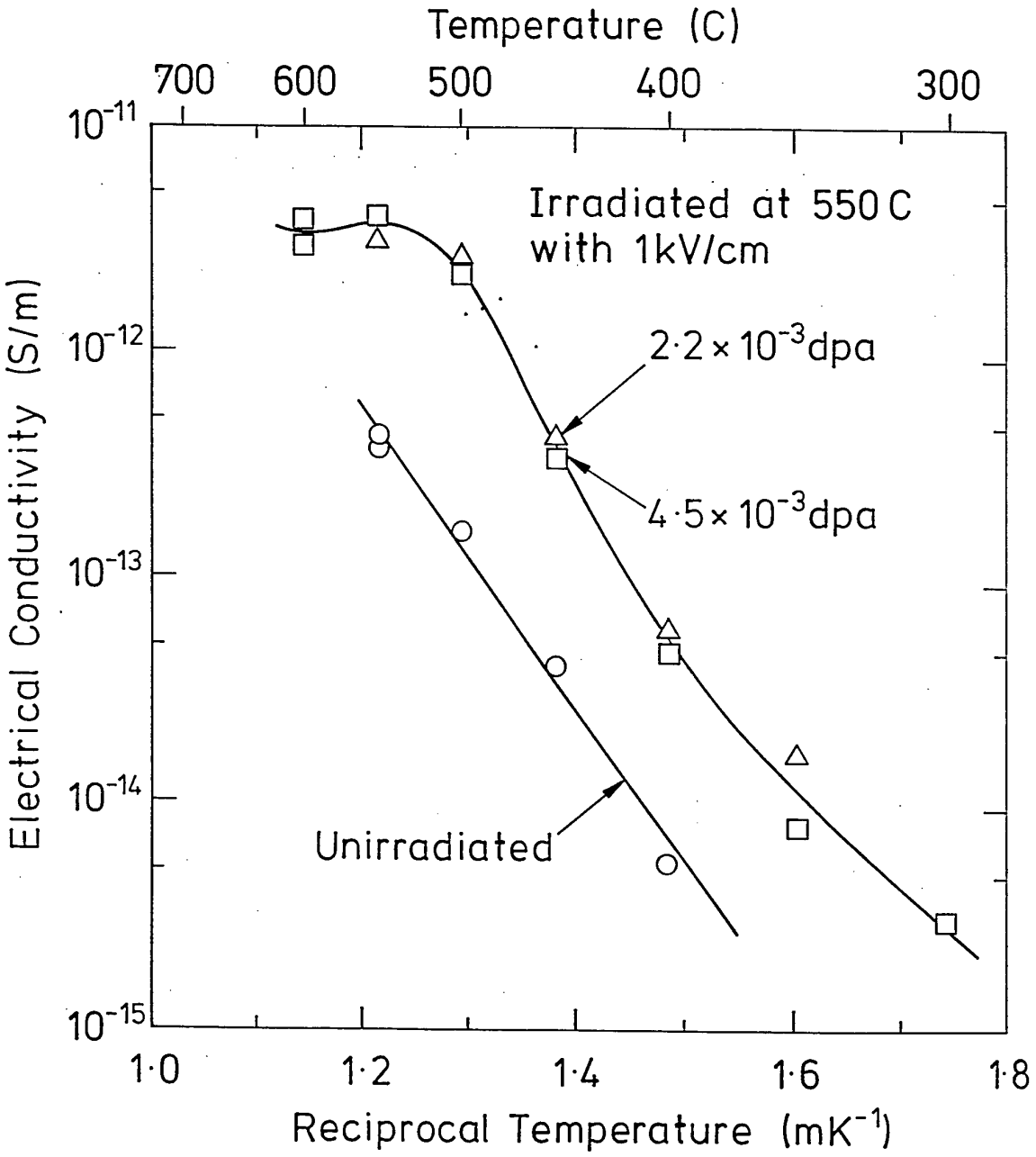

Fig. 7.
The intrinsic electrical conductivity as a function of temperature after 10Mev proton irradiation.